

Tunable Geometric Decoupling Mechanisms for Phased Array Coils

S. P. Bhatia¹, F. J. Robb², Y. Guan², and M. P. McDougall¹

¹Magnetic Resonance Systems Lab, Texas A & M University, College Station, TX, United States, ²G.E. Healthcare, Aurora, OH, United States

Introduction: After their introduction by Roemer *et al* [1], phased array coils have become standard in clinical MR imaging. The development of array coils for small animal MRI is of increasing interest. Field strengths of 4.7T and higher are especially suited for small animal work because of the high SNR offered at these field strengths. Isolation preamplifiers are expensive and not ubiquitous at the field strengths typically employed (4.7T, 9.4T, etc). Therefore most small animal array coil designs typically employ a combination of geometric decoupling to decouple adjacent elements [2-7] and additional techniques, such as capacitive [8] and transformer [9] decoupling to decouple non overlapping elements. Consequently, in the absence of

isolation preamps, optimized geometric decoupling is particularly important. In addition, isolation preamps cannot be used to decouple the elements of transmit arrays. This paper presents “tunable” geometric decoupling between array elements using two methods of implementation. The first is a decoupling paddle that changes the area of overlap and thus the amount of mutual inductance between adjacent elements. The second is a variable overlap mechanism where a portion of one overlapping element is a sliding structure to change the area of overlap. These mechanisms allow the coil-to-coil decoupling to be adjustable and provide a straightforward mechanism for optimizing the overlap area without the tedious process of soldering and resoldering. In addition, the adjustable decoupling is useful when operation is required over a wide range of loading conditions - for example, to collect loaded and unloaded Q measurements. The capabilities of the variable decoupling methods were tested by acquiring S_{21} network analyzer measurements over a range of loading conditions. The effects of adding these mechanisms on two elements arrays was assessed with regard to SNR and field pattern by acquiring images of a homogeneous phantom with and without the decoupling mechanisms in place.

Methods: A two element array (A1) was constructed with square loops of dimensions 6 x 6cm using strips cut from 0.125 inches wide annealed copper (thickness=0.25mm) (Fig 1). For adjusting the amount of decoupling between the two adjacent elements, a flux blocking paddle, similar to that introduced by Hoult [10] was used to control the “open” surface area of the overlap, and thus the mutual inductance. A second similar two element array (A2) was constructed with the variable length tunable decoupling mechanism (Fig 2). The mechanism is based on a concept similar to the trombone-style birdcage coil introduced by Xu and Tang [11] and used frequently by our lab [12]. Two nesting sizes of copper rods were used. 4mm length of larger copper rods (OD=3/32”, Wall thickness=.014”) were cut and attached to the fixed portion of the element to act as a sheath. Smaller copper rods (OD=1/16”, Wall thickness=.014”) were attached to the movable portion of the element copper and slid into the larger copper rod sheaths. With this mechanism, the overlap area between the adjacent elements can be adjusted. A third similar standard two element array that did not incorporate any of the tunable decoupling mechanisms was constructed for comparison purposes. The overlap between the two elements of this array was optimized and fixed on the bench for a 8 x 14 x 15cm cubical phantom filled with 6mM CuSO₄.

S_{21} bench measurements were collected using an RF network analyzer 8712ES (Agilent Technologies, Paulo Alto, CA) from the two arrays with adjustable decoupling as a function of their adjusting mechanism for two different loading conditions (0.1M NaCl and 6mM CuSO₄). To verify the ability of the paddle to control the decoupling by changing the area of overlap, the elements were matched and tuned to 50 ohms and the decoupling measurements were collected at different positions of the paddle at intervals of 2mm for the two different loads. For verification of the ‘variable length’ mechanism to control the decoupling by changing the area of overlap, measurements were collected at different positions of overlap at intervals of 0.5mm. Axial images were acquired from individual elements of all three coil arrays on a 4.7T/33cm scanner supported by a Varian Unity Inova console (spin echo, TR/TE=300/30msec, matrix=128x128, FOV=100mm, st=3mm, N_w=2). G.E. feedboards were used for transmitting/receiving signal from the coil. The SNR of each of the images was computed using a histogram method well suited to surface coil images, in which the voxels containing signal over a given threshold were considered signal and the noise region was user-selected on the image.

Results & Discussion: Fig 3 (top) shows the S_{21} measurements for varying positions of the decoupling paddle for the two loading conditions. Fig 3 (bottom) shows the S_{21} measurements for varying positions of the “variable length” decoupling mechanism for both loading conditions. Note in both cases how the optimization occurs at appreciably different positions of the paddle and the ‘variable length’ for each of the loads, verifying the desired “tunability” of decoupling. Fig 4 shows all images acquired from each individual element of the three array coils. Note that the images acquired from the arrays with tunable decoupling mechanisms show no distortion or significant differences from the field patterns of the standard array. Table 1 shows the normalized SNR comparisons between the images acquired. From the table it is evident

that no significant loss (less than 3%) was observed in the SNR of elements of the coil with the addition of the tunable decoupling mechanisms. Given the straightforward “tunability” of decoupling using these methods, future work will include incorporating these mechanisms into higher count array coils and small animal arrays.

References: [1]Roemer et al; MRM 1990, 16(2):192–225; [2] Keil et al; Proc ISMRM 2008;16:1; [3] Beck et al; Review of scientific instruments 2001;Vol 72(11), 4292-4294; [4] Ullmann et al; Proc ISMRM 2004,16:10; [5] Beck et al; Magnetic Resonance Materials in Physics, Biology and Medicine 2002;13:6; [6] Oduneye et al; Proc ISMRM2008;16:1 [7] Gareis et al; NMR Biomed. 2007;20:9; [8] Nascimento et al; Proc ISMRM 2008;16:1 [9] Zhang et al; Proc ISMRM 2004;11:1 [10] Hoult et al., MRM 1984;1 :339-353; [11] Xu et al., MRM 1997; 37:5 :168-172 [12] McDougall et al., Proc ISMRM 2001; 1092

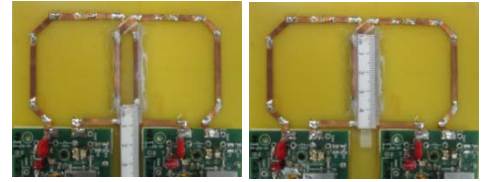


Fig.1: Two element array A1 with decoupling paddle

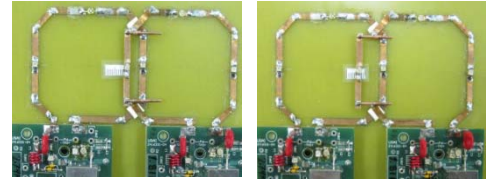


Fig.2: Two element array A2 with ‘variable length’ decoupling

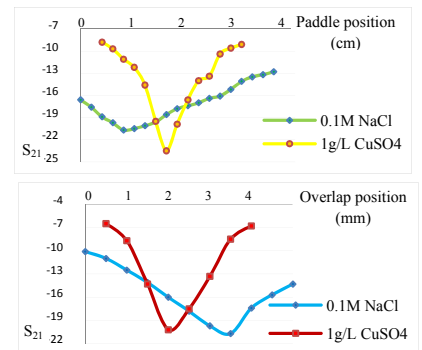


Fig 3: (top) S_{21} vs. paddle position for the array A1 with two different loads. (bottom) S_{21} vs. overlap length for array A2 with two different loads

Fig.4: Axial Images of a cubical phantom taken from each individual element of (top) Array A3; (center) Array A2; (bottom) Array A1

	SNR (Left element)	SNR (Right element)
A3	1	1
A2	0.979	0.987
A1	0.986	0.999

Table 1: Relative SNR of array coils